

Development of Low Temperature Melt Growth Process for Bulk YBCO Superconductors

Roland Loh*

HiTc Superconco Inc., PO Box 128, Lambertville, NJ 08530, USA

(Received 11 November 1995; accepted 17 January 1996)

Abstract: A class of low temperature melt processed bulk high temperature superconductors and methods of making the same are provided. In this work, the ReBaCuO materials were melted and treated by changing the partial pressure of oxygen gas rather than by changing the temperature. The low temperature ‘gas’ melt process eliminates intermediate phases thus enhancing links between grain boundaries, reduces the thermal stress thus minimizing the micro-cracks, and results in a homogenous microstructure because the gas gradient is much less than the temperature gradient. © 1998 Elsevier Science Limited and Techna S.r.l.

1 INTRODUCTION

A weak link between the grain boundaries, misaligned crystals and lack of flux pinning all contribute to the low magnetic force and low critical current of bulk ReBaCuO (YBCO as an example in this study) high temperature superconductors. The objective of this work is to develop fabrication methods for ReBaCuO materials with designed microstructure to overcome these problems.

Recent studies of YBCO materials pointed to two major issues: creating pinning centres and eliminating weak-links between grain boundaries. It has been reported that some defects may be the pinning centres. Until fine 211 inclusions were introduced by the melt-texture-growth process, high pinning strength and high critical current density were observed in YBCO materials.^{1,2} Flux pinning may be effective by two ways: first, the defects around the 211/123 boundary, such as dislocation, stacking fault, and second, the magnetic pinning—a further pinning caused by the different induction generated in 123 superconducting matrix and 211 nonsuperconducting phase.³ However, the weak-link can be caused by impurity phases, micro-cracks, or high-angle misalignment of the

crystals.⁴ In order to overcome the weak links of grain boundaries, many studies have been done, such as the following.

1. Melt Texture Growth process. The crystals with small angle grain boundaries have parallel *c*-axes and *a*–*b* planes slightly rotated around the *c*-axes.
2. Neutron or far-infrared irradiation treatment. The critical current, J_c in a Josephson junction can be enlarged when irradiated by electromagnetic waves having a frequency corresponding to the energy gap of electrode superconductors and power in a certain range. But this kind of enhancement works only for grain boundary functions as Josephson junction at very low temperature (4.2 K).⁵
3. Doping silver. Doping silver improves not only the mechanical properties but also critical current. Silver can enhance the diffusion, improve the grain alignment, and provide conductive paths between grains. The optimum silver content in doped YBCO bulks is based on between tunneling (SIS type)-silver decreases the insulating barrier and proximity (SNS type)-silver increases the normal metal layer thickness.⁶
4. Magnetic grain alignment.

*Present address: Owens Corning Tallmadge Technology Center, Tallmadge, OH 44278-2232, USA.

5. Reducing superconducting bulk size. The Josephson current across grain boundary weak links in polycrystalline YBCO superconductors causes the transport critical current density to increase noticeably when the cross sectional area of the superconductors are reduced.

In conclusion, abnormally large crystals, fine 211, silver or other inclusions and crystal alignment seem to be the three key points in microstructure design for YBCO superconductors. In order to obtain this kind of microstructure, the high temperature melt texture growth (MTG) and its derivative methods, such as melt powder melt growth (MPMG), laser zone melting, tube drop melting, contactless melting growth, seed melt growth, and magnetic grain alignment have been applied to YBCO bulks.

The critical current of the above processed materials demonstrated high enough for practical application, such as $10\,000\text{ A/cm}^2$ in 1 Tesla field at 77 K. These test results have been somewhat deceptive. The tests generally relied on induced magnetization measurement and further calculation of the critical current value by Bean's model. Therefore, these test data did not give enough information about the intergranular component of the critical current. Actually, the MTG materials exhibited large intragranular current but not intergranular current.

In addition, materials with abnormally large crystal microstructure have many intrinsic problems, including aligned micro-cracks, low mechanical strength and toughness, poor thermal shock resistance. In order to make a strong-link of grain boundary by superconduct–nonsuperconduct–superconduct (SNS) junction, the non-superconducting layer must be as thin as possible to the coherence length of the 123 superconductor. This is hard to obtain since the coherence length of the YBCO materials is only about 24 Å in the a , b direction, and 6 Å in the c direction. As a matter of fact, it is almost impossible to eliminate the phase segregation in YBCO materials by any of melt-texture-growth processes.

2 EXPERIMENT

In order to solve the above mentioned problems, we designed a new microstructure for the YBCO superconductor, and developed new processes to achieve this microstructure. Our microstructure for YBCO superconductors is that crystals are short range (not long range) aligned, well developed (not

abnormally large) and with high density of defects. In order to reach the above microstructure we have carried out the following four processes:

2.1 High-pinning crystal preparation

YBCO rod was hung vertically in a furnace and heated rapidly until the rod became partially molten. The rod was further quenched and soaked at about 1000°C , then cooled slowly in oxygen. This is a typical MTG process except no contamination due to the contactless melting of the materials. Finally, the MTG rod was pulverized into fine granules.

2.2 Pinning phase purification (3P) process

The above granules were cooled to liquid nitrogen temperature, a permanent magnet drum was pushed toward the granules inducing magnetization ($-M$). Then the magnet drum was pulled away from the granules reversing the magnetization ($+M$). An attractive force due to the trapped field was thus created. Granules with high pinning were attracted beneath the poles of the magnet and adhered magnetically to the magnet drum. These granules in a size of single crystal or pseudo-crystal were collected finally by thermal de-pinning.

2.3 Cryo-magnet crystal orientation method

The phase purified granules respond strongly in a magnetic field at 77 K caused by pinning effect. Therefore, forming these granules in a magnetic field at low temperature (77 K) created crystal

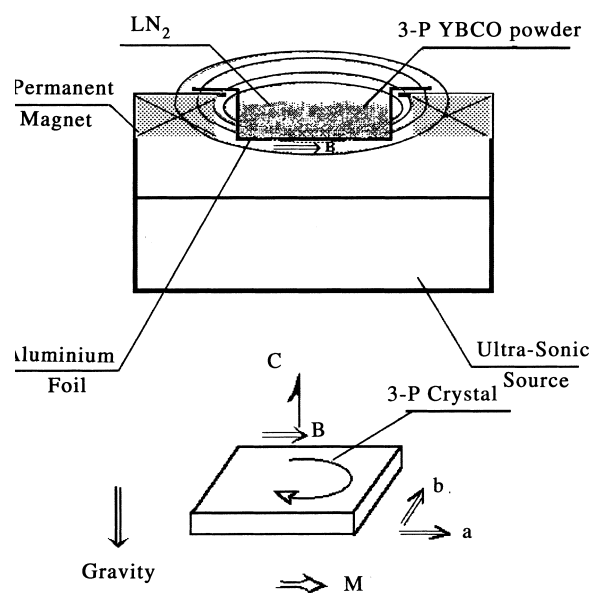


Fig. 1. Illustration of cryo-magnetic orientation field and force.

oriented bulks. A cryo-magnet crystal orientation facility is illustrated as Fig. 1. Direct magnetic field trapping of 3-P granular may be conducted by two ways: field cooling (FC) or zero field cooling (ZFC). It was reported by Houston group that in low magnetization field the trapped field for FC is larger than that for ZFC. Therefore, all of our experiments were based on FC: the 3-P granular were put in the field and then cooled by liquid nitrogen below its superconducting transition temperature. The 3-P crystals are plate-like which are well developed in a - b plane. Therefore, the gravity force can be also served to align crystal along c -axis. A magnetic field B was applied in the direction parallel to the a - b plane. The 3-P crystals were vibrated by an ultra-sonic source. A magnetic moment M of crystal which was induced by the magnetic field B oriented the crystals along the c -axis. This alignment reinforced the gravity c -axis alignment. The alignment was maintained after the liquid nitrogen was evaporated, and the materials were consolidated by isostatic pressing with the holder (a thin aluminium foil) at room temperature.

2.4 Low temperature melt growth (ltmg) process

The isostatic pressed samples were pre-fired at 920 °C in air. The samples were heated to a higher temperature (but less than 1000 °C) and soaked for 10–30 min. The samples were partially melted by changing the atmosphere from air to a low partial oxygen pressure. This is based on that the incongruent melting point of YBCO material varies as a

function of the oxygen partial pressure of the atmosphere. The incongruent melting point is about 950 °C at 0.001 atm of oxygen, 1015 °C at 0.29 atm of oxygen (air), and 1030 °C at 1 atm of oxygen.⁷ The ratio of the O₂/Ar depends on the temperature and varies from 0% to 20%. The samples were soaked at that temperature and atmosphere for 10–100 min depending the size of the sample. Then the samples were quenched by changing the atmosphere to pure oxygen or/and by reducing the temperature. Finally, the samples were cooled very slowly for moderately crystal growth.

In order to evaluate the relationship between process parameters (such as melt temperature, melt oxygen pressure, quench oxygen pressure, duration of crystal growth) and the quality of the materials (such as grain size, grain alignment, phase, defect and density) these factors are evaluated according to an experiment design currently as part of Phase II work.

3 RESULT AND DISCUSSION

The XRD of a typical made 3P crystals is shown on Fig. 2. Only well developed 123 crystals and 211 phase were detected. The test proved that the 3-P crystals were not contaminated by low melting point phases, such as BaCuO₂. This provides a chemically clean grain boundary for the later sintered bulks.

The ratio of orientation in c -axis of the magnet oriented samples is the average 001 peaks over

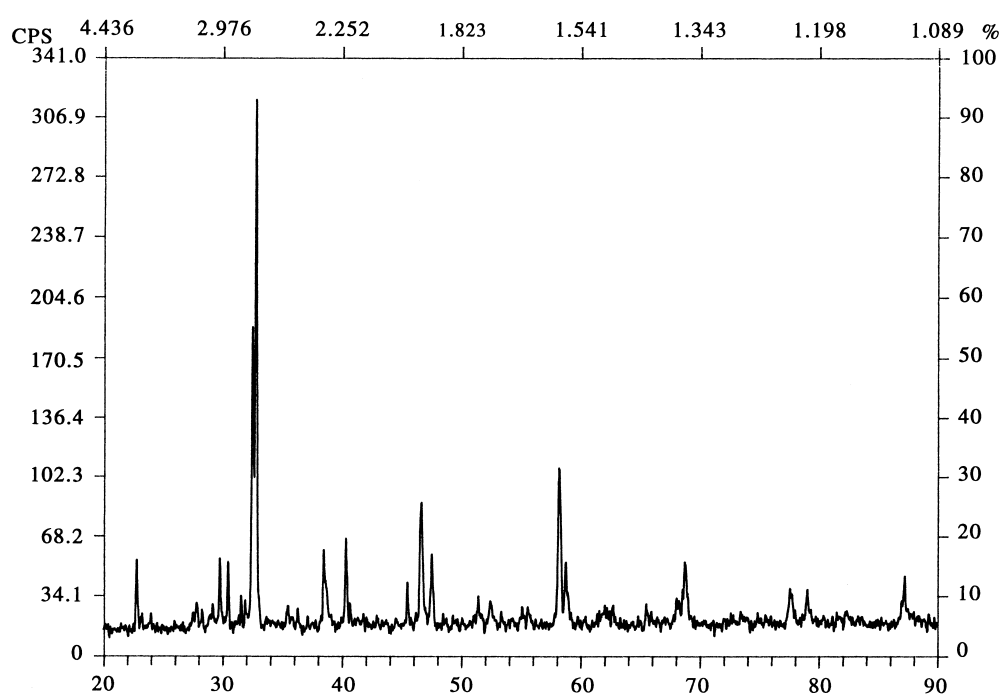


Fig. 2. Diffraction pattern of 3P crystal by XRD.

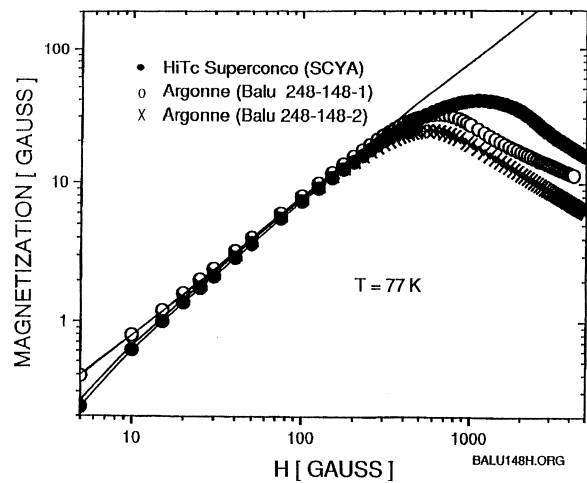


Fig. 3. Magnetization measurement of 3P sample at 77 K.

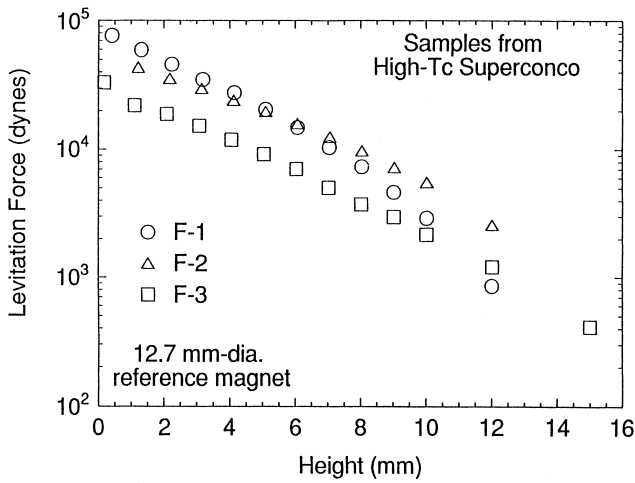


Fig. 4. Levitation force measurement.

the average hkl peak normalized intensity, and is estimated about 80% based on the XRD data tested by Rutgers. This is achieved by using a permanent magnet of which the magnetic strength is only few hundred Gauss.

Figure 3 shows the magnetization data on a sample made from 3P crystals. The straight line, without data points shows the Meissner limit, i.e. the magnetization if the materials were perfectly diamagnetic. The 3P sample is as good as the other best melt-textured YBCO samples and has a higher peak magnetization value.

In order to compare sample F1 prepared by LTMG with sample F2 & F3 prepared by HTMG for magnetic bearing application, the levitation forces were measured by Argonne National Laboratory. Figure 4 shows that the sample F1 has the best performance.

Samples have been examined by SEM and TEM after the LTMG process. Instead of ion milling for one specific area, samples have been ground to thin edge particles and examined carefully to find the inclusions and grain boundaries characterization.

The microstructure and phase distribution by LTMG is much more uniform than that by MTG process. TEM showed that the LTMG sample contains high density of {110} twin planes with an average spacing about 100 nm (Fig. 5). The TEM images are taken with the electron beam nearly parallel to the [001] direction. In this direction, the twin planes appears as lines in $\langle 110 \rangle$ directions. This two-dimensional defects may be the main flux

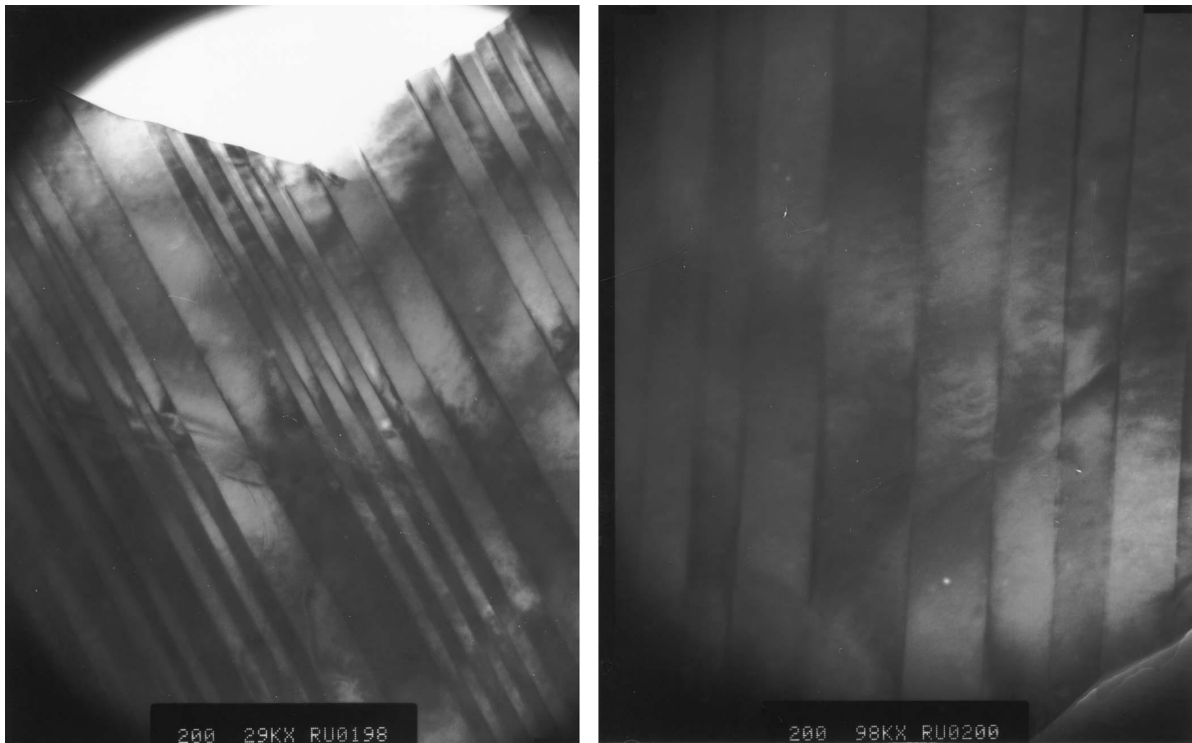


Fig. 5. (110) twin plane observed by TEM.

pinning centres for high J_c which is similar to YBCO thin film.

The MTG and its derivative processes induce non-uniform heating. Even for small sample, the surface reaches the maximum temperature, the inside may not reach above the peritectic reaction temperature. Since the microstructure and phase distribution depend on maximum heating temperature and duration near this temperature, a non-equilibrium mixture of phases are always resulted. Besides, large temperature gradient is necessary for crystal growth in a preferred orientation. While in the low temperature melt growth process, the YBCO materials are melted by 'gas' instead of 'temperature'. The gas gradient is much less than the temperature gradient. Partial healing of the grain boundaries (grain boundary coupling) during liquid phase sintering at low oxygen pressure and low temperature was carried out. The low partial oxygen pressure atmosphere may eliminate the intermediate phases thus enhance links between grain boundaries. Besides, at low temperature, the oriented crystals are still well developed because the grain growth rate is higher at low partial oxygen pressure than at a high one.

4 CONCLUSION

The primary experiment and test result show that the bulk YBCO superconductor processed by low temperature melt growth differs from other MTG materials in a number of significant ways: less contamination due to the low oxygen pressure

sintering and due to the original high pure pinning phase powder made by phase purification process; crystal oriented due to the pre-orientation process; homogeneous macro- and micro-structures due to the homogeneous temperature and atmosphere distribution (both determining the melt point of the materials) which essentially solved the de-mixing of chemical phases and the deformation often found in regular melt texture growth processes.

ACKNOWLEDGEMENTS

This work is supported by NASA under contract # NAS1-19884. The author wishes to thank Dr John Hull, Argonne National Laboratory for his help in magnetic force measurement, Dr Lu Ping, University of Rutgers for his help in SEM and TEM, and stimulating discussions with them.

REFERENCES

1. JIN, S., *Appl. Phys. Lett.*, **52** (1988) 2074–2076.
2. MURAKAMI, M., *Jpn J. Appl. Phys.*, **28** (1989) 1189–1194.
3. HUGHES, D., Flux pinning mechanisms in type-II superconductors. *Phil. Mag.*, **30** (1974) 293–305.
4. MATSUSHITA, T., *IEEE Trans. Appl. Supercond.*, **3**(N1) (1993) 1045–1048.
5. TAKEYA, J., *IEEE Trans. Appl. Supercond.*, **3**(N1) (1993) 1165–1167.
6. MILLER, J., *Appl. Phys. Lett.*, **54** (1989) 2256–2258.
7. IDEMOTO, Y., Melting point of superconducting oxides as a function of oxygen partial pressure. *Jpn J. Appl. Phys.*, **29**(N12) (1990) 2729–2731.